

Supporting Information

Photocatalytic Degradation of Water Contaminants in Multiple Photoreactors and the Evaluation of Reaction Kinetics Constants Independent of Photon Absorption, Irradiance, Reactor Geometry and Hydrodynamics

Ivana Grčić^a and Gianluca Li Puma^{b*}

^a University of Zagreb, Faculty of Chemical Engineering and Technology, Marulicev trg 19, 10000 Zagreb, Croatia.

^b Environmental Nanocatalysis and Photoreaction Engineering, Department of Chemical Engineering, Loughborough University, Loughborough, LE11 3TU, United Kingdom .

* Corresponding author: Environmental Nanocatalysis and Photoreaction Engineering, Department of Chemical Engineering, Loughborough University, Loughborough, LE11 3TU, United Kingdom. Tel.: 0044(0)1509-222510; fax: 0044(0)1509-223923. E-mail address: g.lipuma@lboro.ac.uk (Prof. G. Li Puma).

Content: **Figure S1 and S2.** Emission spectra of UV lamps. **Figure S3.** Schematic representation of the geometry of the annular photocatalytic reactor. **Figure S4.** Forward photon flux emerging from the outer wall of PR1 at different catalyst concentrations and levels of irradiance. **Figure S5.** Results of the modeling of the photocatalytic oxidation of oxalic acid in PR1 with different model assumptions. **Table S1.** Photoreactors dimensions and lamp specifications. **Table S2.** Reaction scheme for the heterogeneous photodecomposition of oxalic acid on TiO₂.

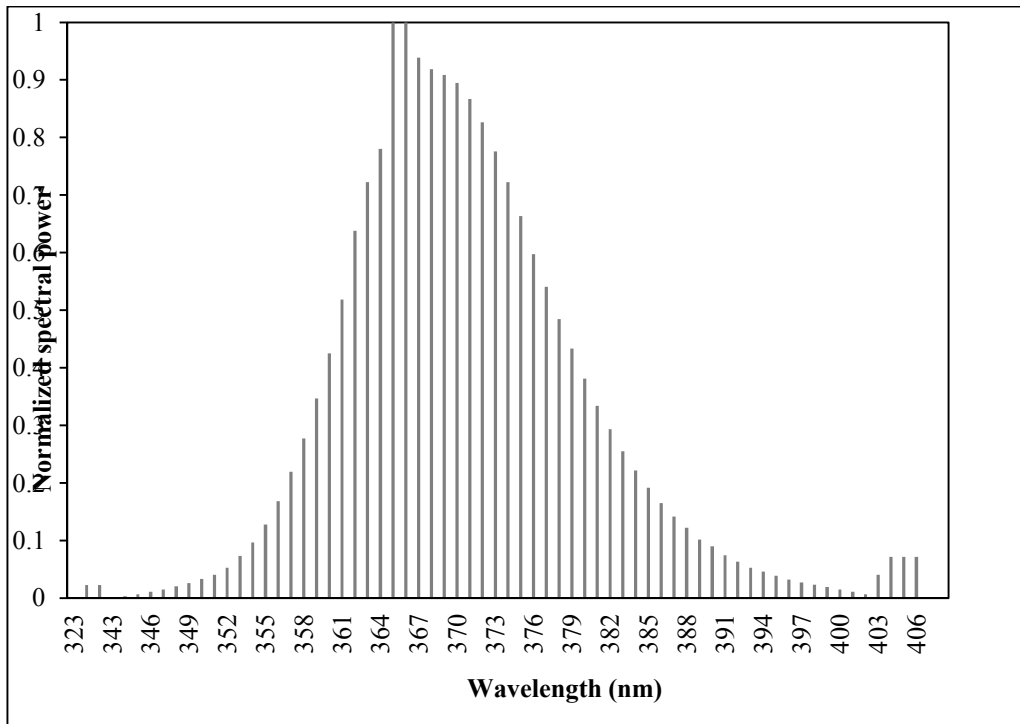


Figure S1. Emission spectrum for blacklight blue fluorescent lamps (Philips blacklight-blue TL 8W/08 F8 T5/BLB lamp).

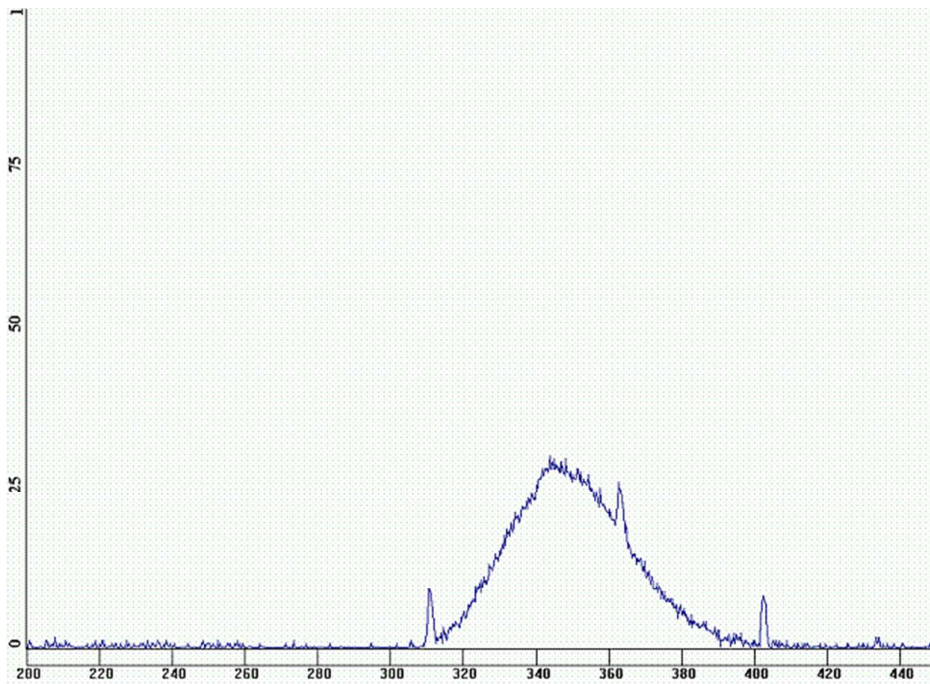


Figure S2. Emission spectrum for UVP Pen-Ray[®] mercury discharge lamp (model 90-0019-04) provided by UVP.

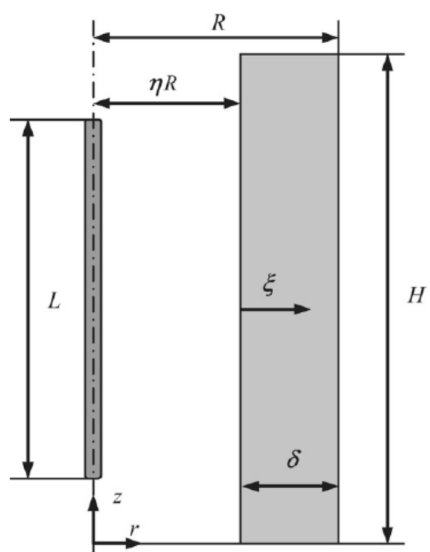
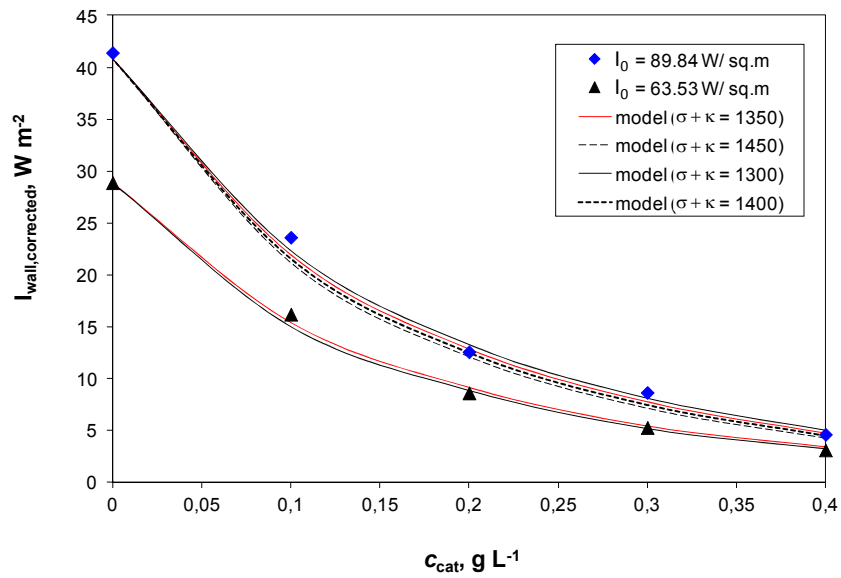
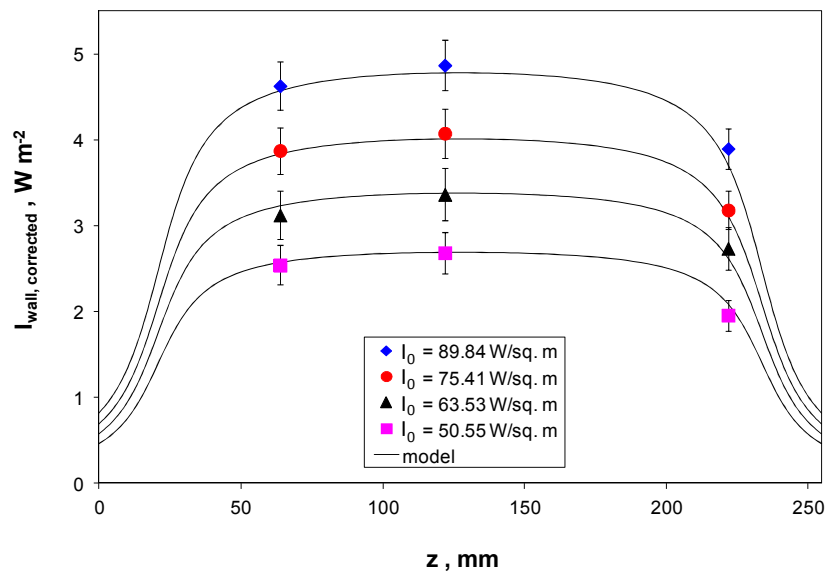


Figure S3. Schematic representation of the geometry of the annular photocatalytic reactor (reproduced from Toepfer et al.¹).



(a)



(b)

Figure S4. Forward photon flux emerging from the outer wall of PR1. (a) At different TiO₂ powder loadings and different levels of irradiance, at $z^* = 0.5$. Lines are the fitting of SFM with $\omega = 0.8617$, symbols are mean values of several measurements. (b) At different positions along the axial direction varying the irradiance. Lines are the fitting of SFM with $\omega = 0.8617$. [TiO₂] = 0.4 g/L.

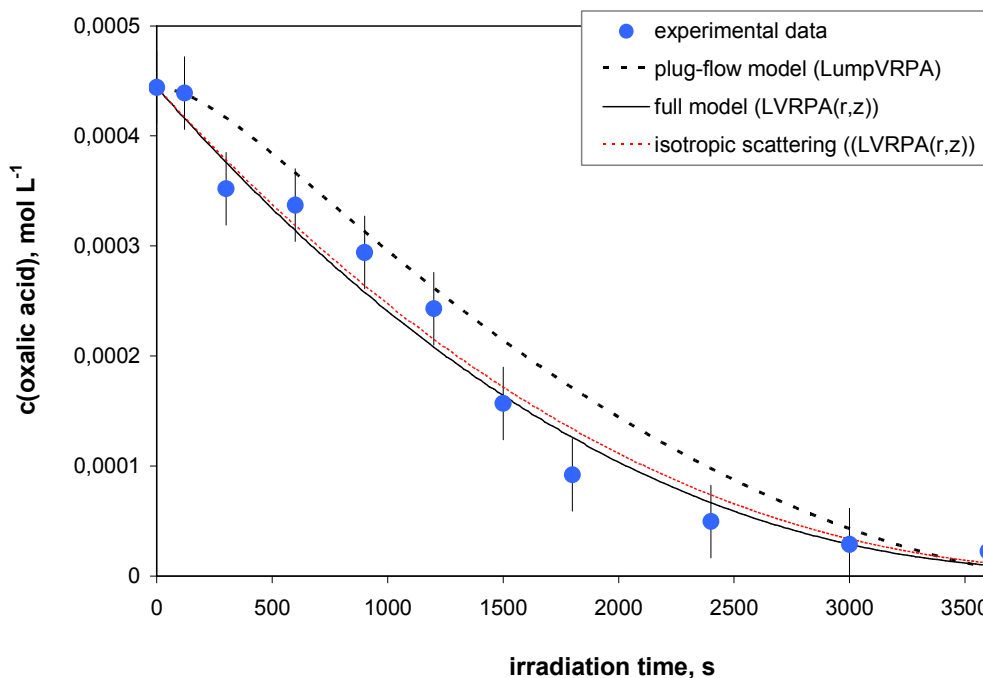


Figure S5. Results of the 5odelling of the photocatalytic oxidation of oxalic acid in PR1 with different model assumptions. pH = 4, [TiO₂] = 0.4 g/L; $I_0 = 89.84 \text{ W m}^{-2}$.

Table S1 Photoreactors dimensions and lamp specifications.

Photoreactor dimensions		PR1	PR2
Length, H	m	0.255	0.095
Inner radius, ηR	m	0.013	0.008
Outer radius, R	m	0.018	0.038
Irradiated volume, V_r	m ³	1.34×10^{-4}	5.00×10^{-4}
Lamp specifications			
Lamp type		Philips TL 8W/08 F8 T5/BLB	PenRay 90- 0019-04
Irradiance at 2 cm from the source	W m ⁻²	86.75	12.55
Bulb length with uniform emission, L	m	0.213	0.0538
Bulb radius, r_l	m	0.00753	0.00475

Table S2. Reaction scheme for the heterogeneous photodecomposition of oxalic acid on TiO₂ according to Pozzo et al.²

<i>Reaction step</i>	
S ₀	Activation (common to both pathways) $\text{TiO}_2 + h\nu \rightarrow \text{h}^+ + \text{e}^-$
S ₁	Adsorption (species A) on dark/illumination conditions $[\text{site}] + \text{C}_2\text{O}_4\text{H}^-_{(\text{sol})} \leftrightarrow \text{C}_2\text{O}_4\text{H}^-_{(\text{ads})\text{A}}$
S ₂	Adsorption (species B) on dark/illumination conditions $[\text{site}] + \text{C}_2\text{O}_4\text{H}^-_{(\text{sol})} \leftrightarrow \text{C}_2\text{O}_4\text{H}^-_{(\text{ads})\text{B}}$
S ₃	Adsorption of oxygen $[\text{site}] + \text{O}_{2(\text{sol})} \leftrightarrow \text{O}_{2(\text{ads})}$
S ₄ , S ₅	Hole trapping (via OH ⁻) and σ bond rupture (fast kinetics) $(\text{OH}^-)_{\text{ads}} + \text{h}^+ \leftrightarrow \text{OH}^\bullet$ $\text{C}_2\text{O}_4\text{H}^-_{(\text{ads})\text{B}} + \text{OH}^\bullet \rightarrow \text{CO}_2\text{H}^\bullet_{(\text{ads})\text{B}} + \text{CO}_2 + \text{OH}^-$
S ₆	Hole trapping (direct) and σ bond rupture (slow kinetics) $\text{C}_2\text{O}_4\text{H}^-_{(\text{ads})\text{A}} + \text{h}^+ \rightarrow \text{CO}_2\text{H}^\bullet_{(\text{ads})\text{A}} + \text{CO}_2$
S ₇	Final mineralization (common to both mechanisms) $\text{CO}_2\text{H}^\bullet_{(\text{ads})} + \text{O}_2 \rightarrow \text{O}_2\text{H}^\bullet + \text{CO}_2$
S ₈	Electron capture $\text{O}_{2(\text{ads})} + \text{e}^- \rightarrow \text{O}_2^{\bullet-}_{(\text{ads})}$
S ₉	Hole–electron recombination $\text{e}^- + \text{h}^+ \rightarrow \text{heat}$
S ₁₀₋₁₂	Complementary (assumed fast) reactions $\text{O}_2^{\bullet-} + \text{H}^+ \rightarrow \text{HO}_2^\bullet$ $2\text{HO}_2^\bullet \rightarrow \text{H}_2\text{O}_2 + \text{O}_2$ $\text{H}_2\text{O}_2 \rightarrow \text{H}_2\text{O} + 1/2 \text{O}_2$

References (Supporting Information)

- (1) Toepfer, B.; Gora, A.; Li Puma, G. Photocatalytic oxidation of multicomponent solutions of herbicides: Reaction kinetics analysis with explicit photon absorption effects. *Appl. Catal. B: Environ.* **2006**, *68*, 171-180.
- (2) Pozzo, R. L.; Brandi, R. J.; Cassano, A. E.; Baltanás, M. A. Photocatalytic oxidation of oxalic acid in dilute aqueous solution, in a fully illuminated fluidized bed reactor. *Chem. Eng. Sci.* **2010**, *65*, 1345-1353